

## FISSILE MASS AND CONCENTRATION CRITERIA FOR CRITICALITY IN GEOLOGIC MEDIA NEAR BEDDED SALT REPOSITORY

Rob P Rechard, Lawrence C. Sanchez

*Nuclear Energy Fuel Cycle Center; Sandia National Laboratories; Albuquerque, NM 87185-0747*

Patrick K. McDaniel, Jacob Hunt, Gabriella Broadous

*Department of Nuclear Engineering; University of New Mexico; Albuquerque, NM*

**Abstract.** This paper describes the fissile mass and concentration necessary for a critical event to occur outside containers disposed in a bedded salt repository. The criticality limits are based on modeling mixtures of water, salt, dolomite, concrete, rust, and fissile material using a neutron/photon transport computational code. Several idealized depositional configurations of fissile material in the host rock are analyzed: homogeneous spheres and heterogeneous arrangements of plate fractures in regular arrays. Deposition of large masses and concentrations are required for criticality to occur for low enriched  $^{235}\text{U}$  enrichment. Homogeneous mixtures with deposition in all the porosity are more reactive at high enrichments of  $^{235}\text{U}$  and  $^{239}\text{Pu}$ . However, unlike typical engineered systems, heterogeneous configurations can be more reactive than homogeneous systems at high enrichment when deposition occurs in only a portion of the porosity and the total porosity is small, because the relationship between the porosity of the fractures and matrix also strongly influences the results.

### I. INTRODUCTION

As with other nuclear facilities, the possibility of fissile mass and concentration causing a self-sustained neutron chain reaction (criticality) must be evaluated for geologic disposal systems both during operations and after closure. This paper discusses the potential of criticality sometime in the future after repository closure of the Waste Isolation Pilot Plant (WIPP), an operating repository in bedded salt in southeastern New Mexico for the geologic disposal of wastes containing transuranic (TRU) radioisotopes from atomic energy defense activities.

In the past, concern about the criticality scenario in TRU waste has been low because of the low initial concentration and mass of fissile material in containers and the natural tendency of fissile solute to disperse during transport, as discussed in 2001 and 2015.<sup>1-3</sup> However, waste destined for WIPP has expanded to include other TRU waste with high initial concentration (although in containers with small

fissile mass).<sup>4</sup> Because of the expansion of the types of waste to be disposed at WIPP, a renewed evaluation of the criticality potential was undertaken.

This re-evaluation for new waste streams has been divided into two parts: (1) physical compaction of the mostly intact Pu containers through salt creep closure of the disposal rooms; and (2) evaluation of hydrologic and geochemical aspects that prevent fissile material from assembling into critical concentrations. The latter part has been further divided into (a) hydrologic and geochemical causes and constraints on fissile mass deposition, and (b) neutronic criteria necessary for a criticality scenario. This paper focuses on the latter aspect, neutronic criteria necessary for the occurrence of the criticality scenario, thus the causes of deposition are not important to the discussion here.

Study of the criticality scenario in a geologic setting is interesting and instructive because behavior of fissile material differs from common expectations. As a stand-alone article, this paper emphasizes this aspect. However, combining this information with the hydrologic and geochemical constraints on concentrating fissile in various geologic settings support the rationale for eliminating the criticality scenario from consideration in performance assessments (PAs) of bedded salt repositories such as WIPP.

This paper updates the previously published calculations for homogenous spherical configurations in the repository and geologic barrier. Homogeneous mixtures are often more reactive (i.e., neutron flux more effectively utilized) than heterogeneous mixtures, especially at high enrichments of plutonium. However, the reactivity may increase in some configurations of lumped, heterogeneous mixtures of fissile material because the neutrons released in fission can migrate through the geologic media/fluid system and miss the large resonances in the non-fissile isotopes. Consequently, idealized heterogeneous mixtures is an important addition to the earlier analysis.

## II WIPP DISPOSAL SYSTEM

### II.A Transuranic Waste

#### II.A.1 General Categories of TRU Waste.

The two primary types of TRU waste originally destined for WIPP are<sup>2</sup> (1) contact-handled transuranic (CH-TRU) waste, which is TRU waste with an external dose rate <0.56  $\mu$ Sv/s (200 mrem/h), and (2) remotely handled transuranic (RH-TRU) waste, which is >0.56  $\mu$ Sv/s but <2.8 mSv/s (1000 rem/h). Currently, 2005 RH containers in 719 canisters have been placed in room ribs and 9 shielded RH-drums have been placed in excavated rooms.

All CH-TRU is disposed in the excavated rooms. The standard waste form of CH-TRU has consisted of a variety of materials contaminated by  $\alpha$ -emitting TRU radionuclides generated from atomic energy defense activities, including inorganics (e.g., iron and

aluminum alloys, equipment, concrete, glass, firebrick, ceramics), organics (e.g., cellulosics, such as paper, cardboard, laboratory tissues, wood, cloth, rubber, plastics), solidified materials (e.g., waste water treatment sludge, cemented liquid waste, inorganic particles and soils), and solvents.

For the CCA-1996, the masses of the two most important fissile materials,  $^{235}\text{U}$  and  $^{239}\text{Pu}$ , were 8.1 and 12.8 metric tons (MT), respectively (Table I). The projected average  $^{235}\text{U}$  enrichment at emplacement for the CCA-1996 was 5.3%. The anticipated uranium enrichment at WIPP has remained less than 6%, except for the CRA-2014 with an estimated enrichment of 15% (Table I). The  $^{239}\text{Pu}$  enrichment was 90% for the CCA-1996 and has remained near that value, except for the CRA-2014 with an estimated enrichment of 76%.

Table I. Current disposed and projected fissile material in 2033 for past re-certifications of WIPP

Radioisotope	CCA-1996 <sup>a</sup> (kg)	Current Estimate as 31 December 2017					
		CRA-2004 (kg)	CRA-2009 (kg)	CRA-2014 (kg)	Disposed (kg)	WIPP Bound <sup>b</sup> (kg)	Total (kg)
<b>Uranium</b>							
$^{233}\text{U}$	202	128	21.5	14.4	0.720	11.9	12.7
$^{234}\text{U}$	121	55.4	49.8	39.0	14.2	284.	298
$^{235}\text{U}$	8 060	2 320	2 080	35 400	203.0	2 370	2 570
$^{236}\text{U}$	10.4	44.4	24.7	84.2	0.0072	9.30	9.30
$^{238}\text{U}$	149 000	646 000	81 300	193 000	52 500	41 900	94 300
Enrichment ( $^{233}\text{U}+^{235}\text{U}$ )	5.3%	0.38%	2.52%	15.5%	0.4%	5.3%	5.6%
<b>Plutonium</b>							
$^{238}\text{Pu}$	113	66.0	85.9	35.1	25.0	32.5	57.4
$^{239}\text{Pu}$	12 800	9 380	8 270	9 260	5 420	6 600	12 000
$^{240}\text{Pu}$	943	420	639	771	367	771	1 140
$^{241}\text{Pu}$	3.83	4.35	4.95	6.44	5.7	9.5	14.7
$^{242}\text{Pu}$	298	3.23	19.3	2060	7.05	59.9	66.9
Enrichment $^{239}\text{Pu}$	90%	95%	92%	76%	93%	88%	93%
$^{239}\text{Pu}$ fissile kg mass equivalent <sup>c</sup>	18 200	11 000	9 670	32 100	5 570	8 180	1, 800
Total (all U and Pu)	172 000	658 000	92 500	241 000	58, 500	52 000	110 600

<sup>a</sup> Ref<sup>1</sup>, Table II

<sup>b</sup> Not scaled; normally PAs scale up WIPP bound inventory to account for future waste streams that fill the repository

<sup>c</sup> The Pu fissile mass equivalence (FME) is the mass of  $^{239}\text{Pu}$  plus various factors of the masses of  $^{238}\text{Pu}$ ,  $^{240}\text{Pu}$ ,  $^{241}\text{Pu}$ ,  $^{242}\text{Pu}$ ,  $^{233}\text{U}$ ,  $^{235}\text{U}$ ,  $^{237}\text{Np}$ ,  $^{241}\text{Am}$ ,  $^{243}\text{Am}$ , and  $^{245}\text{Cm}$ . The mass is usually expressed in grams (i.e., fissile gram equivalence or FGE), but here we use kilograms.

#### II.A.2. Excess Non-Pit Plutonium

As part of the 1991 Strategic Arms Reduction Treaty (START I) with Russia to dismantle ~80% of strategic nuclear weapons, the US Department of Energy (DOE) identified ~51.7 MT of surplus Pu in various stages of manufacturing at several sites for disposition in a 1996 Programmatic EIS. Although DOE preferred to directly dispose this excess Pu, DOE relented and agreed in the 1997 record of decision to fabricate ~34 MT into mixed oxide (MOX) fuel to be consistent with plans in Russia. The other ~17.7 MT were to be immobilized and disposed. In the 2007 notice of intent to produce a Supplemental EIS,

~4 MT of unirradiated fuel of the 17.7 MT was set aside for non-defense research.<sup>5</sup> The remaining 13.7 MT of Pu, included 7.1 MT of Pu from weapon pits (which would require extra processing to convert to MOX), 6.0 MT non-pit Pu unsuitable for producing MOX fuel, and ~0.6 MT of miscellaneous Pu.<sup>5</sup> Disposition of 13.1 MT of Pu in lanthanide borosilicate glass and 34 MT of Pu as MOX (and subsequent disposal of the resulting spent nuclear fuel) was included in the license application for the proposed Yucca Mountain repository.<sup>6</sup> After the Yucca Mountain repository was halted in 2010, DOE decided in

2011 to process the ~0.6 MT of miscellaneous Pu and send it to WIPP.

In 2012, DOE proposed, and in 2016, DOE selected disposal of the 6.0 MT of non-pit Pu inventory at WIPP and subsequently added it to the WIPP inventory (see Table I, Current as of 31 December 2017);<sup>4</sup> however it has not yet been shipped. Because bounding estimates were used in CCA-1996, and because estimates for CRA-2004 and thereafter greatly decreased the  $^{239}\text{Pu}$  inventory, the disposal of 6.6 MT does not represent an increase in  $^{239}\text{Pu}$  over that originally planned in 1996 (Table I).

#### II.A.3 General and Pu Waste Form Concrete

Concrete is present in the WIPP repository both as structural components and encapsulating waste. Cement in concrete does not have a fixed composition, but the major cement components are  $\text{SiO}_2$ ,  $\text{CaO}$ ,  $\text{MgO}$ ,  $\text{Al}_2\text{O}_3$ ,  $\text{Na}_2\text{O}$ , and  $\text{Fe}_2\text{O}_3$ . For general concrete, two cement compositions were used, both defined in SCALE (1) composition specified by the US Nuclear Regulatory Commission (NRC), and magnesium (Mg) composition.

The 6.6 MT non-pit Pu metal is assumed oxidized to  $\text{PuO}_2$  and mixed with a cement-like material and  $\text{H}_2\text{O}$  to form concrete but without any aggregate. A simplified cement composition was used for the waste form here that consisted of 65%  $\text{SiO}_2$ , 22%  $\text{MgO}$ , and 13%  $\text{Al}_2\text{O}_3$  with a density of 2840 kg/m<sup>3</sup> (or 58.5%, 19.8%, and 11.7% including 10%  $\text{H}_2\text{O}$ —Table II). The waste form cement components were selected to increase reactivity to be conservative for criticality analysis; the cement proportions were selected to be reasonably consistent with common cement compositions. The concentration of Pu in the waste concrete mixture is 185 kg/m<sup>3</sup>.

Table II. Element weight percent in various materials

Element Oxides	NRC Concrete <sup>a</sup>	Mg Concrete <sup>a</sup>	Waste Mixture	Culebra Dolomite <sup>b</sup>
$\text{SiO}_2$	72.09	9.01	58.50	1.55
$\text{CaO}$	6.16	31.66		29.39
$\text{MgO}$		15.62	19.80	21.08
$\text{Al}_2\text{O}_3$	6.42	1.50	11.70	0.26
$\text{Fe}_2\text{O}_3$	2.00	0.80		0.22 <sup>c</sup>
$\text{K}_2\text{O}$		1.13		0.09
$\text{Na}_2\text{O}$	3.91	0.19		0.10
$\text{TiO}_2$		0.25		
$\text{Mn}_3\text{O}_4$		0.07		
$\text{SO}_3$		0.50		3.3
$\text{H}_2\text{O}$	8.94	2.95	10.0	
$\text{CO}_2$ or 1000°C		38.58		
Ignition Loss				44.03
Total	99.51	102.25	100.00	100.00
Density ( $\rho^{\text{grain}}$ )	2300	2420	2250	2820

<sup>a</sup>SCALE

<sup>b</sup>Ref<sup>7</sup>, Table IV-4; WIPP-12 at 246.7 m depth

<sup>c</sup>Reported as  $\text{FeO}$

#### II.A.4 Depositional Form of Pu Used

The repository average plutonium mixture that is disposed at WIPP is typically ~90% enriched in  $^{239}\text{Pu}$  (Table I). However, the non-pit Pu enrichment was set at 100%  $^{239}\text{Pu}$  for the criticality calculations described herein. The assumed 100% enrichment increases reactivity but not excessively so. Plutonium that deposits in the either the repository or the geologic barrier is modeled as plutonium dioxide ( $\text{PuO}_2$  with  $\rho_g = 11460 \text{ kg/m}^3$  and 88% of density as  $\text{Pu}^{\text{IV}}$ ).

#### II.A.5 Depositional Forms of U Used

Based on the WIPP inventory, the uranium enrichment was modeled as 5% or 20% enriched (Table I), though an enrichment of 93% was used occasionally for comparison to  $^{239}\text{Pu}$ . Uranium is modeled as uranium dioxide in and around the repository ( $\text{UO}_2$  with  $\rho_g = 10\,970 \text{ kg/m}^3$  and  $\text{U}^{\text{IV}}$  88%wt of density).

Uranium deposition in the dolomite, above the repository, is also modeled as Rutherfordine ( $\text{UO}_2\text{CO}_3$  with  $\rho_g = 5724 \text{ kg/m}^3$  and  $\text{U}^{\text{VI}}$  72%wt of density) because it is the thermodynamically stable form for  $\text{U}^{\text{VI}}$  in a carbonate solution.

### II.B. Geologic Characteristics of WIPP Disposal System

#### II.B.1. Castile Formation

The lowest strata discussed here is the Castile Formation (Fig. 1). Within the land-withdrawal boundary of WIPP, a pressurized brine reservoir has been intersected in the fractured Anhydrite III layer of the Castile by exploratory borehole WIPP-12.<sup>2</sup> Hence, the WIPP PAs assume (a) pressurized brine reservoirs exist in the Castile beneath a portion of the repository and (b) Castile brine could enter the repository through a new exploratory borehole in the next 10 000 years. In the criticality calculations, the composition of the Castile brine used here is from exploratory borehole ERDA-6 (Table III).<sup>9</sup>

Table III. Composition of Culebra, Salado, and Castile brines near WIPP.<sup>9</sup>

Constituent	Brine Concentration (mM or mole/m <sup>3</sup> )		
	Culebra (Air Intake Shaft)	Salado (G - Sep)	Castile (ERDA - 6)
Sodium ( $\text{Na}^{+1}$ )	600	4110	4870
Magnesium ( $\text{Mg}^{+2}$ )	21	630	19
Potassium	8.3	350	97
Calcium ( $\text{Ca}^{+2}$ )	23	7.68	12
Boron ( $\text{B}^{+3}$ )	2.8	144	63
Chloride ( $\text{Cl}^{-1}$ )	567	5100	4800
Sulfate ( $\text{SO}_4^{-2}$ )	77	303	170
Bromine ( $\text{Br}^{-1}$ )	0.37	17.1	11
Bicarbonate ( $\text{HCO}_3^{-1}$ )	1.1	0.01	16
Ionic strength	800	6700	5300
Calculated total dissolved solids (kg/m <sup>3</sup> )	43.2	337	305

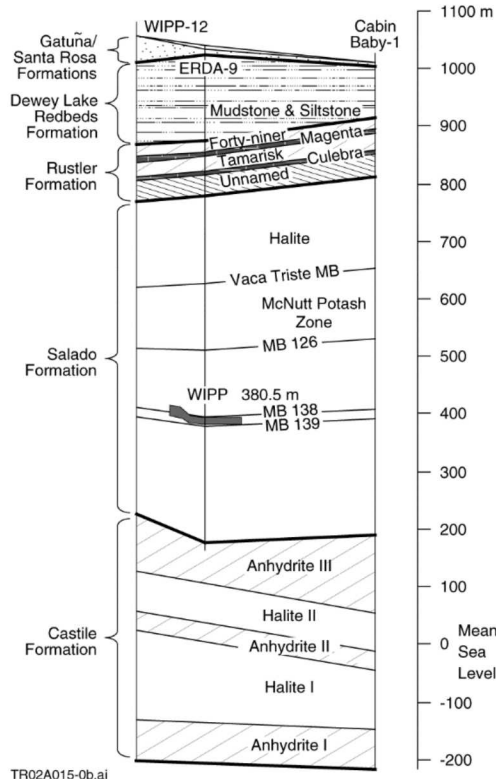


Fig. 1. Stratigraphy above and below the WIPP repository<sup>1</sup>, Fig. 4

### II.B.2. Salado Formation

The 600-m-thick Salado Formation, which overlays the Castile, hosts the WIPP repository 658 m below the surface. The intergranular Salado brine has substantially more magnesium and potassium than the Castile brine (Table III).<sup>a</sup>

### II.B.3. Culebra Dolomite Member of Rustler Formation

The Rustler Formation overlies the Salado. The 7.3-m thick Culebra Dolomite Member of the Rustler Formation is the most likely pathway for transport of radionuclides away from the repository after an inadvertent human intrusion because it is the most permeable saturated stratigraphic unit (Fig. 1). The Culebra consists mostly of dolomite with minor amounts of gypsum, quartz, and clay.

The Culebra has been divided into four units near the WIPP repository.<sup>2</sup> The uppermost unit, Culebra Unit 1, averages 3.0 m in thickness but is not transmissive with only a small number of fractures that occur along bedding planes. The middle Culebra Units, 2 and 3, are similar except for the extent of fracturing. The fractures in both units typically extend less than 5 cm and connect numerous vugs. Originally, the vugs were anhydrite pockets that hydrated to gypsum during sedimentation; subsequent dissolution of gypsum left the vugs. The fractures in both

units are either open or gypsum-filled, with apertures up to 2 mm wide. Culebra Unit 2 is about 1.6 m thick; Culebra Unit 3 is about 1.2 m thick. The lowermost Culebra Unit 4 is typically 1.5 m thick near the repository.

The total (or bulk) porosity of the Culebra Dolomite Member of the Rustler is the sum of the vug, fracture, and matrix porosities, that is

$$\phi_{\text{Culebra}}^{\text{total}} = \bar{\phi}^{\text{vugs}} + \bar{\phi}^{\text{frac}} + \bar{\phi}_{\text{Culebra}}^{\text{matrix}} (1 - \bar{\phi}^{\text{vugs}} - \bar{\phi}^{\text{frac}})$$

The micro-vug porosity  $\bar{\phi}^{\text{vugs}}$  of the lower 3 units is  $\sim 0.05$ . Based on tracer tests in 1996, the advective fracture porosity  $\bar{\phi}^{\text{frac}}$  of the lower 3 units is log-uniformly distributed between  $10^{-4}$  and  $10^{-2}$  with a median of  $10^{-3}$ ,<sup>10</sup> Fig. 2<sup>3</sup>. An advective porosity of  $4 \times 10^{-2}$  is used here as a bounding value. The fracture spacing (2B), presumably between conductive bedding planes, is log-uniformly distributed between 0.1 and 1 m,<sup>10</sup> Fig. 2<sup>4</sup> but a slightly smaller value of 0.05 is used here. The intact matrix porosity  $\bar{\phi}_{\text{Culebra}}^{\text{matrix}}$  is distributed between 0.10 and 0.25 with a median of 0.16.<sup>1</sup>

Based on these values, the total porosity is between 15% and 32% (Table IV). At short times, deposition of fissile material in the matrix porosity through diffusion will not be substantial. Also, much of the micro-vug porosity is not directly accessible to flowing fractures and, thus, unavailable for fissile deposition at short times and travel distances. Hence, any fissile deposition would mostly be in the fractures.

Table IV. Total porosity of Culebra dolomite for various fracture, vug, and matrix porosities

Vugs (%)	Fracture (%)	Matrix (%)	Equivalent Matrix and	
			Vugs (%)	Total (%)
5	4.0	10	15	18
		16	20	24
		21	25	28
		25	29	32
1.0	1.0	10	15	15
		16	20	21
		21	25	26
		25	29	30
0.1	0.1	10	15	15
		16	20	20
		21	25	25
		25	29	29

<sup>a</sup> Herein, brine refers to an aqueous solution with total dissolved solids (TDS) greater than 30 kg/m<sup>3</sup>. For comparison, brackish water refers to

solutions with TDS between 3 and 30 kg/m<sup>3</sup>; fresh water refers to solutions with TDS less than 3 kg/m<sup>3</sup>.

### III. CALCULATION OF CRITICAL CONCENTRATION AND MASS FOR HOMOGENOUS SPHERE

#### III.A. SCALE

Although numerous criticality experiments have been performed in ideal material, criticality experiments with common geologic material have not. Consequently, we used the SCALE v6.2.1 modular code system and the 238 group ENDF-VII.1 group criticality library of tabulated cross-sections, which is provided in the standard release. Within SCALE, the XSDRN module was used, which deterministically solves the one-dimensional Boltzmann transport equation in spherical coordinates.

This core sphere was surrounded by a spherical reflector with a radius 2 m greater than the core to approximate a reflector of infinite extent ( $r^{core} + 2$  m). The spherical reflector has the same composition as the idealized sphere of fissile, rock, brine mixture, but the fissile mass component is replaced with additional fluid.

Five parameters describe the homogeneous model (and are common to the heterogeneous model described in §V): (1) void fraction not occupied by geologic material (matrix porosity in Table II), (2) fraction of the void that is occupied by fissile waste material ( $0 < f_{matrix}^{fissile} < 1.0$ ), (3) fluid filling pores, (4) enrichment of fissile material, (5) grain density of mineral form of fissile material ( $\rho_{grain}^{fissile}$ ).

#### III.B. Fissile-Water Mixture

In describing the possibilities of homogeneous mixtures of fissile material in the literature, the behavior of fissile material immersed in pure water is often presented as the fissile mass versus the fissile concentration. For criticality to occur in a 100% enriched  $^{239}\text{Pu}/\text{H}_2\text{O}$  mixture, the  $^{239}\text{Pu}$  mass must be greater than 0.5 kg and the  $^{239}\text{Pu}$  solid concentration must be greater than 7 kg/m<sup>3</sup> (Fig. 2). But, the minimum concentration is much larger in Castile and Salado brines: a factor of 5 and 7 larger than water for Cl<sup>-1</sup> concentrations of 4800 and 5100 mM, respectively. The minimum mass is a factor of 9 and 13 larger than water, respectively. As the concentration of fluid decreases, the concentration of  $^{239}\text{Pu}$  approaches the solid density of pure  $^{239}\text{Pu}$  at a mass of ~6 kg.

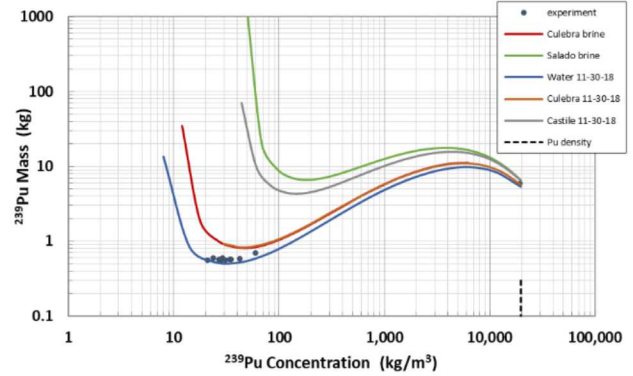


Fig. 2. Comparison of calculated and measured critical masses of plutonium in a homogeneous, spherical shape in  $\text{H}_2\text{O}$  and WIPP brines.<sup>1</sup> Fig. 5; 8, Fig. 7

For criticality to occur in a 5% enriched  $^{235}\text{U}/\text{H}_2\text{O}$  mixture, the  $^{235}\text{U}$  mass and solid concentration must be  $>1.8$  kg and  $>15$  kg/m<sup>3</sup>, respectively. For 93% enriched  $^{235}\text{U}/\text{H}_2\text{O}$  mixture, the  $^{235}\text{U}$  mass and solid concentration must be  $>0.8$  kg and  $>12$  kg/m<sup>3</sup>, respectively (Fig. 3).

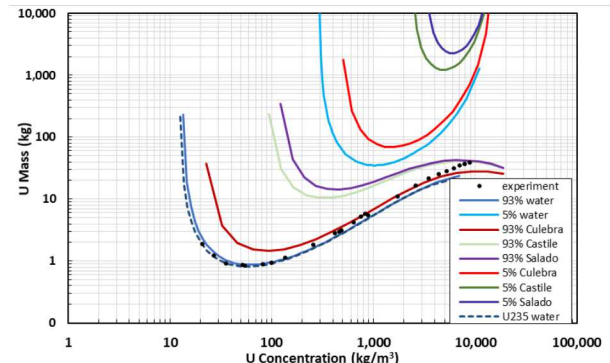


Fig. 3. Critical mass and concentration of 5% and 93% enriched uranium in spherical shape in water and WIPP brines

The minimum critical mass of  $^{239}\text{Pu}$  or  $^{235}\text{U}$  is not usually used in the rationale arguing for omitting the criticality in performance assessments because the mass of fissile material collected in a region of geologic material is dependent on time (e.g., flow rates), unless a geometrical constraint on the maximum mass or volume exists. Rather, the concentration limit is used since the limit is mostly independent of time and more easily compared to geologic processes such as dissolution, adsorption, and precipitation.

## IV. CRITICAL LIMITS FOR FISSIONABLE HOMOGENEOUS SPHERE IN VARIOUS MATERIALS

### IV.A. Fission Critical Limits in WIPP Salt

The critical concentration and mass is about  $140 \text{ kg/m}^3$  ( $\sim 20\%$ wt in dry Halite) and 500 kg, respectively, for 100% enriched  $\text{PuO}_2$  thoroughly mixed/deposited in Halite with 5% porosity saturated with Salado brine (Fig. 4). The critical mass decreases to 134 kg at an unrealistic concentration of  $1930 \text{ kg/m}^3$  (53%wt) for an unrealistic Halite porosity of 20%. All the curves end abruptly when the Halite porosity is completely filled with the fissile material (Fig. 4).

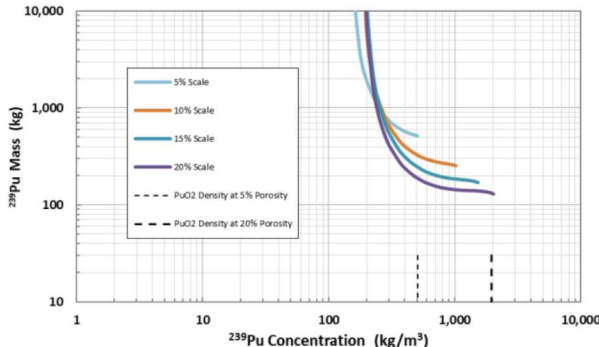


Fig. 4. Critical concentration is  $\sim 140 \text{ kg/m}^3$  ( $\sim 20\%$ wt) and 500 kg for  $\text{PuO}_2$  100% enriched in  $^{239}\text{Pu}$  in Halite saturated with Salado brine with 5% matrix porosity.

Although uranium disposed at WIPP is typically 5% enriched in  $^{235}\text{U}$ , an enrichment of 20% was used here to display the critical limits because of the extreme high mass and critical concentration at 5% enrichment with homogeneously mixed with Halite. Furthermore, CRA-2014 anticipated 15% enrichment. The critical concentration of 20% enriched  $\text{UO}_2$  is  $175 \text{ kg/m}^3$  (6.3%wt) at 10% porosity. The critical minimum mass of 28 000 kg  $^{235}\text{U}$  is only slightly less than the 29,570 kg currently planned to be disposed at WIPP plus 25% decay of  $^{239}\text{Pu}$  over  $10^4$  years ( $2570 \text{ kg } ^{235}\text{U} + 0.25(12\,000 \text{ kg } ^{239}\text{Pu})$ )—Table I).

### IV.B. Plutonium Critical Limits in Homogeneous Culebra Dolomite

For a homogeneous mixture of 100% enriched  $^{239}\text{PuO}_2$  in Culebra dolomite saturated with Culebra brine, the minimum concentration limit for criticality is  $3 \text{ kg/m}^3$  at 10% total available porosity. The minimum mass limit is 2.5 kg for 10% porosity (Fig. 5). These limiting values are the same as those used previously for the CCA-1996.<sup>1</sup> A critical concentration of  $\sim 3 \text{ kg/m}^3$  in the Culebra requires deposition conditions that would produce at least a low-grade ore (1200 ppm or 0.12 %wt at 16% porosity in  $2850 \text{ kg/m}^3$  dolomite with  $\text{PuO}_2$  density of  $11460 \text{ kg/m}^3$  filling 10% of pores)

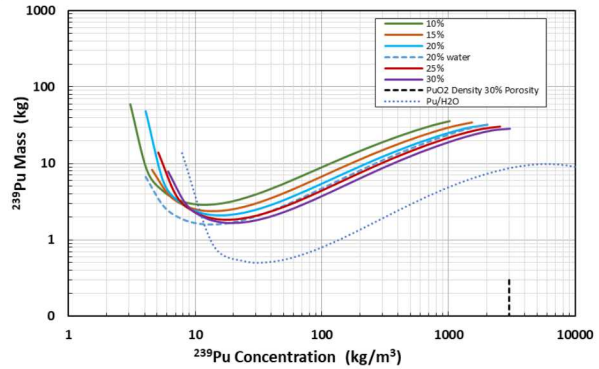


Fig. 5. Critical concentrations and masses for 100% enriched  $^{239}\text{Pu}$  deposited as  $\text{PuO}_2$  in homogeneous Culebra dolomite saturated with Culebra brine and total porosity between 10% and 30%.

### IV.C. Uranium Critical Limits in Homogeneous Culebra Dolomite

For uranium, as Rutherfordine ( $\text{UO}_2\text{CO}_3$ ) (5%  $^{235}\text{U}$ ), the minimum concentration is  $\sim 8 \text{ kg/m}^3$  and 29 kg at 16% total porosity available for deposition, when expressed as  $^{235}\text{U}$ . The minimum concentration is  $\sim 160 \text{ kg/m}^3$  and the minimum critical mass is 580 kg for 16% total porosity available for deposition, when expressed as total uranium (Fig. 6).

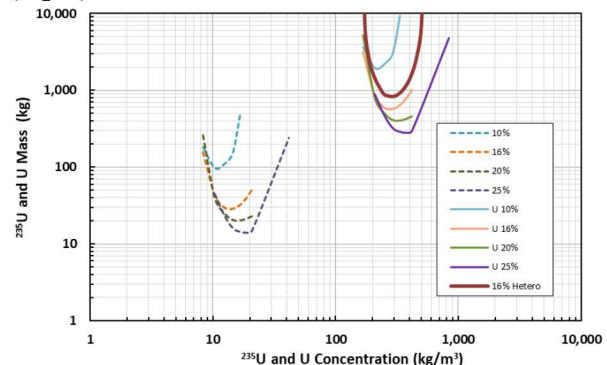


Fig. 6. Critical limits for 5% enriched  $^{235}\text{U}$  as Rutherfordine in homogeneous Culebra dolomite at variable porosity saturated with Culebra brine.

### IV.D. Fission Critical Limits in Concrete

In water and Salado brine, NRC-concrete is more reactive than Mg-concrete. The minimum critical concentration varies between 3 and  $4 \text{ kg/m}^3$  (Fig. 7). Increasing the concrete porosity from 10% to 20% with pure water as a fluid, also increases reactivity. However, increasing the concrete porosity with Salado brine as the fluid, does not influence the critical mass since the large amount of chloride and boron compensates for the additional available hydrogen in the pores. However, the critical concentration is greatly influenced. The behavior of concrete (composed of  $\text{SiO}_2$ ,  $\text{CaO}$ , and  $\text{MgO}$ ) is most similar to Culebra dolomite, which is dominated by  $\text{Ca}^{+2}$  and  $\text{Mg}^{+2}$ .

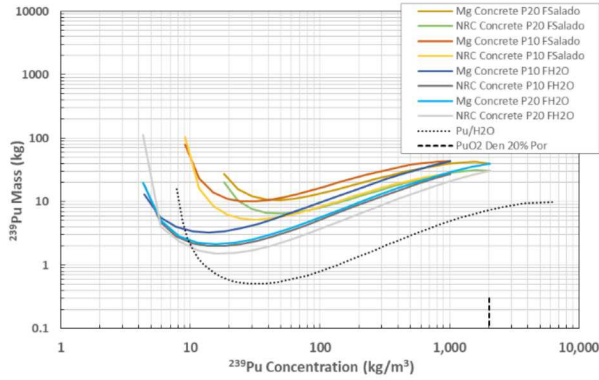


Fig. 7. Critical limits of 100% enriched Pu in various concrete mixtures with water and Salado WIPP brine

#### IV.E. Fissile Critical Limits in Rust

For fissile material mixed with iron corrosion products of the drums and metals in the waste within the repository (here modeled as goethite  $\alpha\text{-FeO(OH)}$ ), the limiting critical concentration in Salado brine is  $26 \text{ kg/m}^3$  (0.87%wt) for 100% enriched  $\text{PuO}_2$  (Fig. 8), and  $45 \text{ kg/m}^3$  and  $1600 \text{ kg/m}^3$  (34%wt) for 93% and 5% enriched  $\text{UO}_2$ , respectively (Fig. 9).

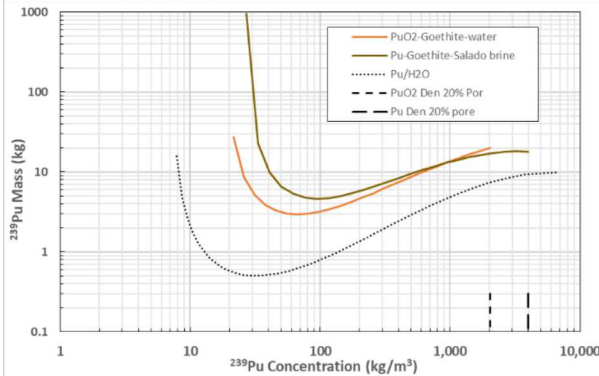


Fig. 8. Critical limits of 100% enriched Pu in goethite at 20% porosity.

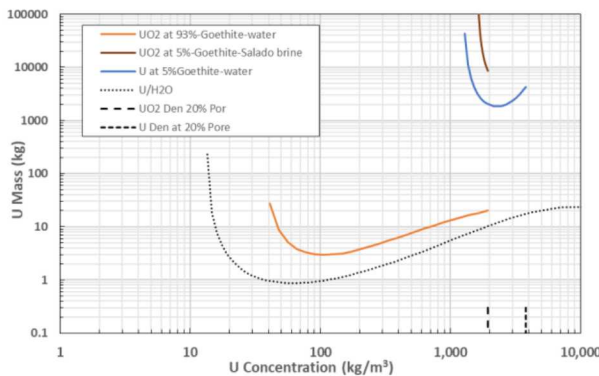


Fig. 9. Critical limits of uranium in goethite at 20% porosity

## V. CRITICAL LIMITS CONSIDERING HETEROGENEITY IN CULEBRA DOLOMITE

### V.A. Modeling Approach for Heterogeneity

As noted in §II.B.3, the Culebra dolomite has an advective porosity along bedding planes and fractures. Furthermore, the matrix porosity may be inaccessible except by diffusion and so fissile deposition may only occur in the fracture porosity. Hence, fissile deposition in the Culebra dolomite may more accurately modeled as heterogeneous. To evaluate the heterogeneity effects, we developed a model of fissile deposition in distinct fractures of the Culebra using a fracture porosity of 4% ( $0.1 < \phi_{frac} < 4\%$ ), small fracture spacing of 0.05 m ( $0.05 \text{ m} < 2B < 1 \text{ m}$ ), and moderate matrix porosity of intact Culebra of 16% ( $10\% < \phi_{matrix} < 25\%$ ). Like the homogeneous model, the core sphere was surrounded by a spherical reflector of the same Culebra dolomite-brine mixture with a radius 2 m greater than the core ( $r^{core} + 2 \text{ m}$ ) (Fig. 10).

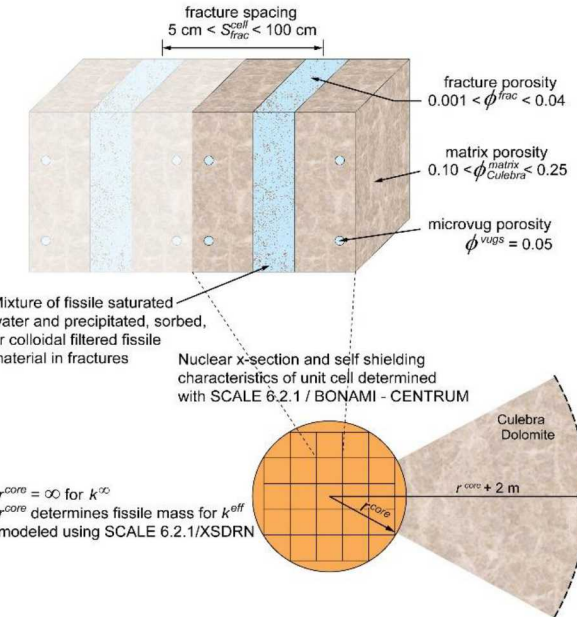


Fig. 10. Model for heterogeneous fracture deposition mixture in Culebra dolomite (a) conceptual model, and (b) infinite and finite extent of unit cells

Besides the 5 parameters for the homogeneous model, the heterogeneous fracture model requires 3 additional parameters: (6) fracture porosity ( $\phi_{frac}^{void}$ ), (7) fraction of the void filled with fissile material ( $0 < f_{frac}^{fissile} < 1.0$ ), and (8) fracture spacing ( $2B$ ).

The spacing between fissile-containing fractures in the Culebra dolomite matrix defined the pitch between unit cells. The unit cells were arranged in a spherical configuration. The nuclear cross-sections for an array of repeating unit cells were processed by the BONAMI and CENTRUM modules to adjust self-shielding and resonance absorption/flux depressions to include small-

scale heterogeneity effects (Fig. 10). The calculations were then performed using the deterministic option, XSDRN module, like the fully homogeneous spherical model but using the nuclear cross-sections that included the heterogeneity effects of the repeating array of fracture unit cells.

### V.B. Plutonium Critical Limits in Culebra Fracture Array

Heterogeneity is influential when the fracture porosity is near 4% and the fracture spacing is reduced to between 0.1 m and 0.05 m. The minimum critical concentration is  $\sim 3.7$  kg/m<sup>3</sup> in a heterogeneous fracture array in the Culebra spaced 5 cm with 18% total porosity (5% vug porosity, 4% fracture porosity, and 10% matrix porosity—Table IV) (Fig. 11). This minimum critical concentration does not differ substantially from the minimum critical concentration from a homogeneous model discussed previously in §IV.B. When the heterogeneous results are more meaningfully compared to a homogenous model with 4% maximum available porosity (since deposition is confined to the fracture porosity) the minimum critical concentrations are similar (Fig. 16).

However, masses are noticeably different. Masses are less for Pu concentrations  $> 20$  kg/m<sup>3</sup> (Fig. 11) when high energy neutrons are more influential than thermal neutrons. However, heterogeneous masses are never less than the homogeneous model when the entire matrix porosity is available for deposition. That is, the maximum pore space for fissile material is 4% in the homogeneous model in Fig. 11 while the maximum pore space for fissile material in Fig. 5 is 25%; hence, the critical masses are larger in Fig. 11.

As expected from the high concentrations of chloride (Table III and Fig. 2), the critical concentration increases for Castile and Salado brines to 12 kg/m<sup>3</sup> at 19% total porosity (Fig. 12).

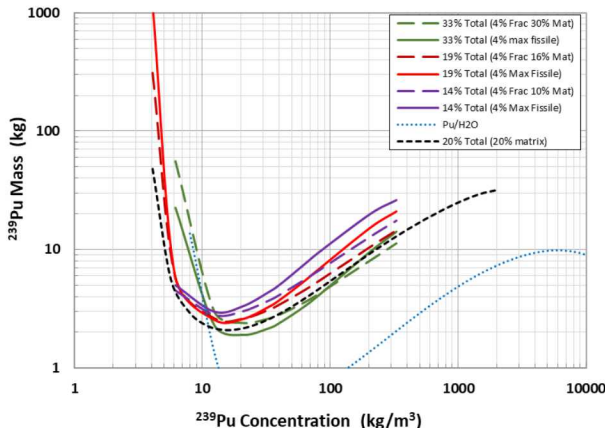


Fig. 11. Critical masses and concentrations of 100% enriched  $\text{PuO}_2$  in the Culebra at variable matrix porosity as homogeneous mixture and as heterogeneous planar fractures at 0.05 m spacing and 4% fracture porosity for deposition.

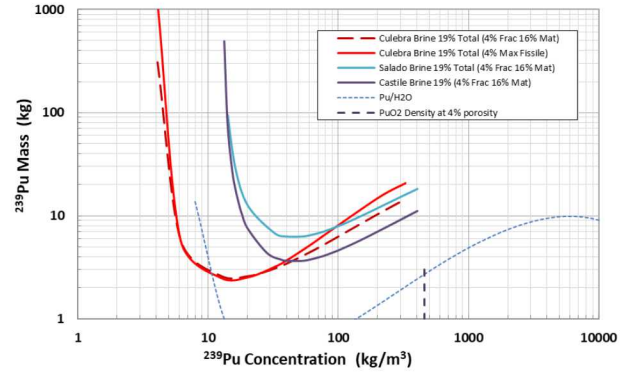


Fig. 12. Critical mass and concentration for 100% enriched  $\text{PuO}_2$  in Culebra dolomite with deposition in 19% total porosity (4% fracture porosity and 16% matrix pores) saturated with Culebra, Castile, and Salado brines

### V.C. Uranium Critical Limits in Culebra Fracture Array

For 93% enriched uranium, the minimum critical  $^{235}\text{U}$  mass is 4.6 kg, and the minimum asymptotic concentration is 6.6 kg/m<sup>3</sup> at 19% total porosity (16% matrix and 4% fracture) (Fig. 13). Note that at high enrichment, the mineral form of the deposited fissile material is unimportant ( $\text{UO}_2$  and Rutherfordine behavior similarly).

At 5% enrichment, the minimum U mass and concentration is 300 kg and 175 kg/m<sup>3</sup>, respectively (29 kg and  $\sim 8$  kg/m<sup>3</sup> as  $^{235}\text{U}$ ) for a homogeneous model of the Culebra where all of the 16% matrix porosity is available for deposition, as presented earlier (Fig. 6). For a homogeneous model of the Culebra with 4% fracture porosity available for deposition of 5% enriched uranium as Rutherfordine is critical only at masses above  $10^4$  kg. At 10% enrichment, the minimum critical mass is 100 kg and the minimum asymptotic concentration is 82 kg/m<sup>3</sup> (3.6%wt) (Fig. 14).

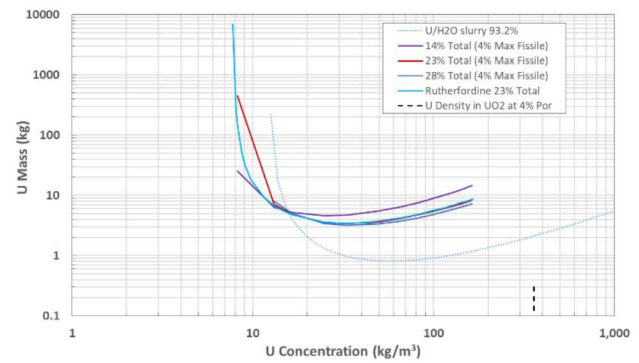


Fig. 13. Critical masses and concentrations of 93% enriched  $\text{UO}_2$  and  $\text{UO}_2\text{CO}_3$  in the Culebra at various matrix porosities as homogeneous mixture and as heterogeneous planar fractures at 0.05 m spacing and 4% fracture porosity for deposition.

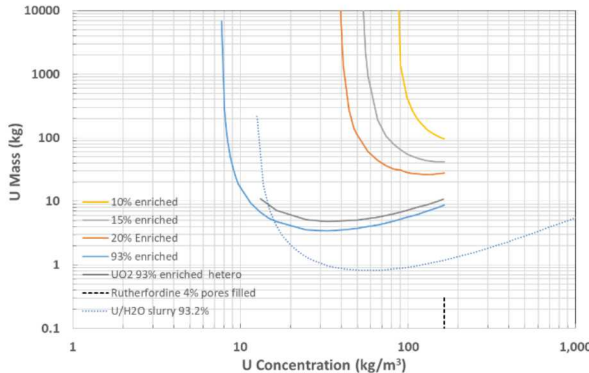


Fig. 14. Critical concentration of  $\text{UO}_2$  and  $\text{UO}_2\text{CO}_3$  at various enrichments in Culebra dolomite with 20% equivalent matrix porosity and 4% fracture porosity available for deposition (23% total porosity)

## VI. CONCLUSIONS

The substitution of WIPP brines for water in a fissile/fluid binary system substantially increases the mass of fissile material necessary to go critical for both  $^{239}\text{Pu}$  and  $^{235}\text{U}$ . Similarly, the addition of geologic media to a fissile/fluid system substantially increases the mass of fissile material necessary to go critical for both  $^{239}\text{Pu}$  and  $^{235}\text{U}$ . The mass of 5% uranium required almost exceeds the amount of U to be placed at WIPP.

The influence on the asymptotic limiting concentration varies. Often it decreases the critical concentration, but for large neutron absorbing salt it increases the critical concentration (Fig. 4).

In previous work, the Culebra dolomite was modeled as homogeneous media with all the porosity available for deposition of fissile material. However, the Culebra dolomite is more accurately modeled as fractured heterogeneous media with deposition primarily in the fractures. A homogeneous model with deposition in all the porosity bounds both the minimum critical concentration and mass of a heterogeneous model. Furthermore, a homogeneous model with deposition in only 4% of the porosity is also bounding except when the total heterogeneous porosity is  $>18\%$  (Fig. 15).

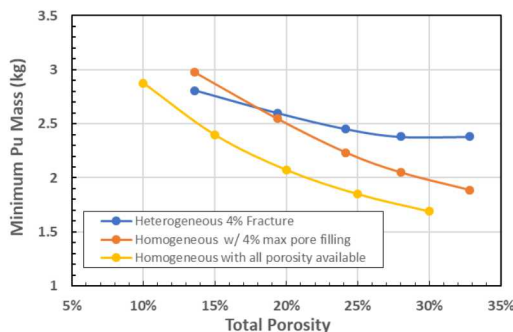


Fig. 15. Critical Pu mass for homogeneous models less than for heterogeneous model with total porosity  $>18\%$  and 4% fracture porosity

The minimum critical concentration bounds for homogeneous models are fairly tight (Fig. 16). For example, the minimum critical concentration of  $3.4 \text{ kg/m}^3$  at  $18\%$  total porosity (minimum porosity in Table IV for 4% fracture porosity) for a fully homogeneous model does not differ substantially from the  $3.8 \text{ kg/m}^3$  minimum critical concentration for a heterogeneous model (nor the  $3 \text{ kg/m}^3$  used previously).

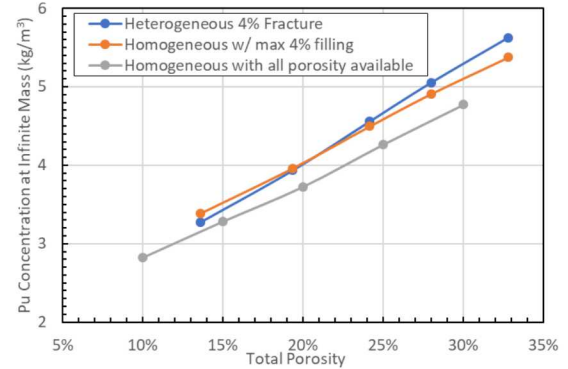


Fig. 16. Minimum Pu critical concentration is  $3.8 \text{ kg/m}^3$  at infinite mass for homogeneous and heterogeneous models at the  $18\%$  minimum total porosity of the Culebra dolomite.

A homogeneous model with deposition in only 4% of the porosity is also bounding at large total porosity but at porosity  $<21\%$ , the minimum critical concentration of a heterogeneous model with 4% fracture porosity is less. Hence, heterogeneity is important when deposition only occurs in a portion of the porosity (here the fracture porosity) and the total porosity is small, even at high enrichment.

Furthermore, the porosity of the geologic media has a strong influence on both the critical mass and the critical concentration in Culebra brine (as apparent from Fig. 16). However, the influence of porosity on the critical mass diminishes for highly saline Salado WIPP brine (Fig. 7).

## ACKNOWLEDGEMENTS

Sandia National Laboratories is a multimission laboratory managed and operated by National Technology & Engineering Solutions of Sandia, LLC, a wholly owned subsidiary of Honeywell International Inc., for the US Department of Energy's National Nuclear Security Administration under contract DE-NA0003525. This paper describes objective technical results and analysis. Any subjective views or opinions that might be expressed in the paper do not necessarily represent the views of the US Department of Energy or the US Government.

## REFERENCES

1. R. P. RECHARD, L. C. SANCHEZ, H. R. TRELLUE and C. T. STOCKMAN, "Unfavorable Conditions for Nuclear Criticality Following Disposal of Transuranic Waste at the Waste Isolation Pilot Plant," *Nuclear Technology*, **136**(1), 99-129 (2001).
2. R. P. RECHARD, "Historical Background on Performance Assessment for the Waste Isolation Pilot Plant," *Reliability Engineering and System Safety*, **69**(1-3), 5-46 (2000).
3. R. P. RECHARD, "Probability and Consequences of Nuclear Criticality at a Geologic Repository--I: Conceptual Overview for Screening," *Nuclear Technology*, **190**(2), 97-126 (2015).
4. DOE (US DEPARTMENT OF ENERGY), "Surplus Plutonium Disposition, Record of Decision," *Federal Register*, **81**(65), 19588-19594 (2016).
5. DOE (US DEPARTMENT OF ENERGY), "Notice of Intent to Prepare a Supplemental Environmental Impact Statement for Surplus Plutonium Disposition at the Savannah River Site," *Federal Register*, **72**(59), 14543-14546 (2007).
6. R. P. RECHARD and C. T. STOCKMAN, "Waste Degradation and Mobilization in Performance Assessments of the Yucca Mountain Disposal System for Spent Nuclear Fuel and High-Level Radioactive Waste," *Reliability Engineering and System Safety*, **122**(2), 165-188 (2014).
7. T. SEWARDS, A. BREARLEY, R. GLEN, I. D. R. MACKINNON and M. D. SIEGEL, "Nature and Genesis of Clay Minerals of the Rustler Formation in the Vicinity of the Waste Isolation Pilot Plant in Southeastern New Mexico," SAND90-2569, Sandia National Laboratories (1992).
8. R. P. RECHARD, L. C. SANCHEZ and H. R. TRELLUE, "Consideration of Nuclear Criticality When Directly Disposing Highly Enriched Spent Nuclear Fuel in Unsaturated Tuff, Part 1: Nuclear Criticality Constraints," *Nuclear Technology*, **144**, 201 (2003).
9. L. BRUSH, H, "Test Plan for Laboratory and Modeling Studies of Repository and Radionuclide Chemistry for the Waste Isolation Pilot Plant," SAND90-0266, Sandia National Laboratories (1990).
10. R. P. RECHARD and M. S. TIERNEY, "Assignment of Probability Distributions for Parameters in the 1996 Performance Assessment for the Waste Isolation Pilot Plant, Part 2: Application of Process," *Reliability Engineering and System Safety*, **88**(1), 33-80 (2005).